A new approach to estimate the performance and energy productivity of photovoltaic modules in real operating conditions

Alain K. Tossa, Y.M. Soro *, Y. Azoumah, D. Yamegueu

*LESEE-2iE, Laboratoire Energie Solaire et Economie d'Energie, Institut International d'Ingénierie de l'Eau et de l'Environnement,
01 BP 594 Ouagadougou 01, Burkina Faso*

Abstract

In this study, a new theoretical approach offering a good prediction of the performance of photovoltaic modules/strings/arrays was developed. The approach implemented in the Matlab/Simulink environment, is based on Levenberg Marquardt (LM) algorithm and was used to estimate the parameters of five electrical models selected among the most used ones. First the problem of initial guess is considered. For parameters initial values, an analysis of six was performed and lead to the choice of the group which offers the best trade-off between accuracy and speed of calculation. To validate the effectiveness of the proposed approach, the five-parameter model (L5P) is used for a comparison with both a deterministic method and two heuristics methods. The results clearly show that, the accuracy achieved with LM method is comparable to the deterministic one, but higher than that of the heuristics methods. Furthermore, the five selected electrical models have been evaluated on four different PV modules technologies. The *I–V* characteristic curves obtained under Standard Test Conditions (STC) by each of them, are compared to the manufacturer data. It was shown that, when the LM algorithm is used, the fives electrical models predict the behavior of the photovoltaic silicon modules with close accuracy. The best trade-off is achieved with L5P model. This result is confirmed by the theoretical estimation of solar energy production performed for three real power plants by using the fives models. The maximum difference between calculated and measured energy is around 14%.
© 2014 Elsevier Ltd. All rights reserved.

Keywords: Levenberg Marquardt algorithm; Photovoltaic module; Energy productivity; Modeling; Outdoor conditions

1. Introduction

This last decade, the enthusiasm of developing countries for renewable energies and especially for the photovoltaic (PV) energy has been strongly increased because of the energy crisis they are facing. In Africa, numerous projects are implemented for both large scale PV plants and stand-alone PV systems. For example, thanks to the recently energy policy adopted in Cape Verde, several PV plants have been installed, the largest one has a power of 5 MWp. In Burkina Faso, a very advanced project is underway for a PV system of approximately 30 MWp. Individual kits are mostly developed for rural population as the rural electrification rate is very low, about 18% according to the International Energy Agency (AIE, 2013). However, as PV modules sold on the market are not tested in natural environmental conditions very often, the performance of these latters is much less than those measured under standard test conditions (STC) and given by the manufacturer (Merten et al., 2008).

* Corresponding author. Tel.: +226 50 49 28 00; fax: +226 50 49 28 01.
  E-mail address: moussa.soro@2ie-edu.org (Y.M. Soro).

Nomenclature

$DeltaE$	relative error *of* the estimated energy
$E_g, E_{g_{ref}}$	gap of the semi-conductor material in the real and reference conditions respectively (eV)
E_{th}, E_{meas}	monthly energy of PV field estimated and measured respectively (kW h)
$ErPmax$	relative error on the maximum power of the module
$f(p)$	modulus of the vector $r(p)$
$G, Gref$	solar irradiation in real and reference operating conditions respectively (W/m^2)
H	Hessian of the function f
$I_o, I_{0_{ref}}$	saturation current in real and reference operating conditions respectively (A)
I_i, Ith_i	measured and estimated currents (A)
$I_{ph}, I_{ph_{ref}}$	photocurrent in real and reference operating conditions respectively (A)
$J(p)$	Jacobian of the vector $r(p)$
K	constant of Boltzmann (1.38×10^{-23} J K^{-1})
LM	Levenberg Marquardt algorithm
$L3P$	three parameters electrical model
$L4P$	four parameters electrical model
$L5P$	five parameters electrical model
$2M7P$	seven parameters electrical model
m	number of points of the IV curve measured under reference conditions

M1DR	single diode electrical model with recombination current in the intrinsic layer i
M2DR	two diodes electrical model with recombination current in the intrinsic layer i
n	ideality factor
NRMSE	normalized root mean square error
NMBE	normalized mean bias *error*
$N_{modules}$	number of identical modules of the PV field,
p	vector of electrical parameters
$Pmax_{th}$	estimated value of the maximum power of PV module (kWp)
$Pmax_{measure}$	measured value of the maximum power of PV module (kW p)
R_s, Rs_{ref}	series resistance in real and reference operating conditions respectively (Ω)
$R_{sh}, R_{sh_{ref}}$	shunt resistance in real and reference operating conditions respectively (Ω)
SD	Standard deviation
T, T_{ref}	solar cells temperature in real and reference condition (K)
T_a	ambient temperature (K)
T_{NOCT}	nominal temperature of the PV cells (K)
$\alpha_{I_{SC}}$	temperature coefficient of the short-circuit current
β_{Voc}	temperature coefficient on the open circuit voltage

Moreover, the energy production is sometimes quite different for module of different technologies of same maximum power is measured under STC. In fact, the module performances are closely related to its intrinsic characteristics such as the absorption, the resistance and the manufacturing process. These latters are greatly influenced (but not in the same way) by the environmental conditions, the temperature and the sun irradiation (solar power and spectrum) (Merten et al., 2008). For example, a high level of irradiation would be beneficial to crystalline technologies whereas amorphous silicon and chalcopyrite based modules have current and voltage mismatch due to material metastable phenomenon (Cañete et al., 2014). It is therefore difficult, but essential to know how to choose, for a given site, the technology that provides the best trade-off between cost and the real performance of the module in a natural environment. One of the major challenges in this choice lies in the mathematical model to be used, in order to precisely predict the performance of photovoltaic modules under real operating conditions.

Many scientists have focused their studies on the modeling of photovoltaic modules and have developed several electric models with different level of complexity. These models differ mainly by the number of diodes, the shunt resistor (finite or infinite), the ideality factor (fixed or variable) and the numerical methods used to determine the unknown parameters (Saloux et al., 2011; Lun et al., 2013; Kulaksiz, 2013; Siddiqui and Abido, 2013; Ma et al., 2014). So far, the results of studies conducted in order to compare different models are still subject of many debates in the scientific community. Then, the key issue to be addressed is "which model can better reproduce the electrical behavior of a given PV module under real environmental conditions?"

The aim of this paper is to propose a new approach based on Levenberg Marquardt (LM) algorithm, which can help choosing the suitable electrical model for a given PV technology. The most used five electrical models are implemented with the same method (LM method). Once the PV module parameters are determined for each model, its energy productivity can be estimated by using the electrical parameters obtained with the best model. The choice of the preferred model is guided by the analysis of statistical errors of each electrical parameters, and by the accuracy of the model. This approach can then be used as a quick and accurate decision tool, not only for the choice of the best electrical model to estimate the energy productivity of a given PV technology, but also for the choice of the best PV technology suitable to climatic and environmental characteristics for a given site.

2. Electrical models of a photovoltaic generator

2.1. Literature review and choice of the electrical model

The electrical behavior of a photovoltaic module is defined by its current–voltage characteristic (Ma et al., 2014; Malaoui and Elmansouri, 2010). The common models generally used to reproduce this characteristic, are based on one diode and two diodes equivalent electrical circuit (Askarzadeh and Rezazadeh, 2012). Recently, other models with recombination current in the intrinsic layer (Merten et al., 2008, 1998; Merten and Andreu, 1998; Muñoz et al., 2012) have been developed especially for amorphous and HIT (Heterojunction with Intrinsic Thin layer) technologies modules. The most electrical models available in the literature are gathered in Table 1.

The choice of an electrical model can be based on several criteria: the calculation speed, the PV technology, the accuracy, etc. Comparative studies of various electrical models have been conducted and have led to several classification based on the module technology and the complexity of the model (Townsend, 1989; Dongue et al., 2012; Karamirad et al., May 2013). Townsend (Townsend, 1989) compared the simulation results obtained with different models to experimental measurements and concluded that the four-parameters model L4P, is the most appropriate one to estimate long-term performance of a photovoltaic module. According to him, this L4P model provides good information with a reasonable computational effort. Karamirad et al. (2013) have also shown that using the artificial neural network (ANN), the L4P model is slightly better than the five-parameter model (L5P). On the other hand, a comparative study of L4P and L5P models by Dongue et al. (2012) has shown that the L5P model strongly agrees to experimental data than the L4P model for mono-crystalline and multicrystalline modules. However, the authors highlighted on the fact that for the multicrystalline module, at low irradiance of about 200 W/m², the L4P model curve is closer to the experimental data than L5P model. Askarzadeh and Rezazadeh (2012) have compared the L5P model and the two diodes seven-parameters model (2M7P) on a commercial silicon solar cell. Their study reveals the better performance of the 2M7P model (accuracy of 0.47% with 2M7P model against 0.44% with L5P model). Other results (Merten et al., 2008; Wolf and Benda, 2013) also show that the model with two diodes are more efficient for both real p–n and p–i–n junctions. Therefore, the thin film solar modules and crystalline type modules, should be better modeled with two diodes models.

As above-mentioned, authors of these studies generally concluded that the greater the number of the model, the more the model is accurate and also the more it is complex. In addition, some results such as those of Townsend (Townsend, 1989) show that, beyond their complexity, models with two diodes present other limits. For example, the model 2M7P does not reproduce the I–V curve as well as other models when the temperature of the cells strongly deviates from the reference temperature (20 °C).

It is now established that there is no clear relation between the PV technology, the environmental conditions and the electrical model. Then, the modeling of a given module requires the comparison of results from different models.

In this paper, five electrical models (L4P, L5P, 2M7P, M1DR and M2DR) will be compared by using the I–V curves measured under Standard Test Conditions (STC) and available in the manufacturer's datasheets.

2.2. Extraction methods of photovoltaic parameters

The extraction of the photovoltaic parameters requires solving of nonlinear equations obtained from the electrical models. After the choice of an electric model, another important problem lies in the extraction method of its parameters. This obstacle is often the cause of rejection of models with two diodes, even though they may be more accurate. Indeed, it is difficult to obtain analytically the optimal parameters of these models. Most of the methods developed and used are graphical, analytical, numerical, heuristics or from artificial intelligence. In Table 2, a non-exhaustive list of the extraction methods is shown.

A comparative study of the methods of Newton–Raphson and LM was conducted by Malaoui and Elmansouri (2010). They compared the ability of each method to reproduce the experimental measurement (I, V) performed on a Schottky diode. The study has shown that the LM method is more accurate and faster. In fact, the LM method is robust and fast because it combines the methods of the gradient descent and the Gauss–Newton (Marquardt, 1963). Furthermore, the assets of the Levenberg–Marquardt method has been proven in many studies (Malaoui and Elmansouri, 2010). It is remarkably well used for different models and domains of physics, so it becomes now a standard for solving non-linear problems by the least square adjustment. For all these reasons, we chose the LM method in this study to extract the parameters of the five models proposed in the previous paragraph.
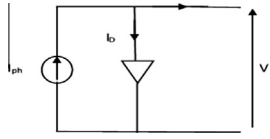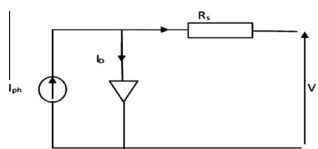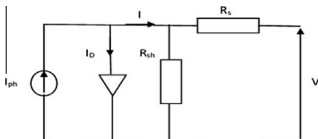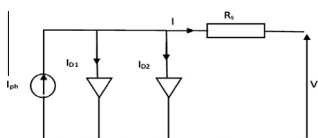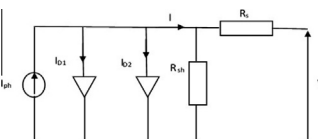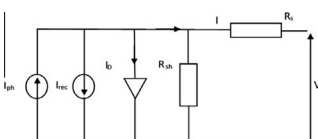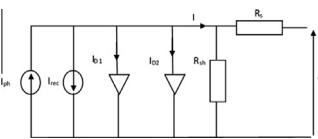
2.3. Initial guesses

An inappropriate choice of initial values of parameters can impact the results. For example, bad initial values could greatly increase the number of iterations and lead sometime to a divergence of the optimization algorithm (Laudani et al., 2014, 2013; Ghani et al., 2013). Below, we briefly present some discussions of the literature on the initial guesses of different parameters that are necessary for the electrical models.

2.3.1. The photocurrent

In most of the studies, the photocurrent (I_{ph}) is approximated by the short circuit current (Ghani et al., 2013, 2013;

Table 1
Summary of electrical models.

Group	Model	Parameters	Equivalent circuit
Single diode electrical models	– Three parameters model (L3P)	I_{ph}, n, I_0	
	– Four parameters model (L4P)	I_{ph}, n, R_s, I_0	
	– Five parameters model (L5P)	I_{ph}, n, R_s, R_{sh}, I_0	
Two diodes electrical models	– Six parameters model (2M6P)	I_{ph}, R_s, n_1, n_2, I_{01}, I_{02}	
	– Seven parameters model (2M7P)	I_{ph}, R_s, R_{sh} n_1, n_2, I_{01}, I_{02}	
Electrical models with recombination current in the intrinsic layer i	– Single diode model (M1DR)	I_{ph}, R_s, R_{sh} n I_0, μ_τ	
	– Two diodes Model (M2DR)	I_{ph}, R_s, R_{sh} n_1, n_2, I_{01}, I_{02}, μ_τ	

Ghani and Duke, 2011; Bai et al., 2014). This assumption is generally accepted for the modeling of PV module or cell because in real devices the series resistance is low while the parallel resistance is high. This parameter is often considered as a good starting point in several refined iterative algorithm (Attivissimo et al., 2013). In this paper, the short circuit current (Isc_{ref}), measured at reference conditions is chosen as the initial value for I_{ph}. When Isc_{ref} is not directly available in an experimental data, its value can be obtained by an interpolation with the experimental data.

$$I_{ph0} = Isc_{ref} \tag{1}$$

2.3.2. The diode ideality factor

In the one-diode models (L4P, L5P, M1DR), the diode represents the diffusion process of charge carriers. A second diode is added in two-diode models (M7P, M2DR), to take into account the space charge recombination current. Many authors (Villalva et al., 2009; Ishaque et al., 2011a, 2011b) generally set the values of diode ideality to 1

Table 2
Summary of the methods used to extract the parameters from electrical models.

Approach	Advantage	Inconvenience	Some methods
Graphical	– Enables a study of natural phenomenon such as aging or seasonal effect (Merten et al., 2008; Merten and Andreu, 1998)	– Requires a lot of measurements on the module	– Variable Illumination Measurement (VIM) (Merten et al., 1998; Muñoz et al., 2012)
		– Leads to inaccurate results if an inaccurate assumption of illumination levels is made	– Analysis of dark current–voltage (Oueriagli, 1992) – Semi-log plots (Sharafa and Akpootu, 2013)
Analytical	– Requires only some key points of the I–V curve (Ishaque et al., 2012)	– Any wrong selected points result in significant error in the parameters to be extracted (Ishaque et al., 2012)	– Lambert W function (Ghani and Duke, 2011)
	– Requires less calculation	– Often consider many approximations which decrease the accuracy	– Study of Bai et al. (2014) – The Taylor's series expansion (Lun et al., 2013)
Numerical	– Needs information on all the points of I–V curve	– Extensive computation	– The secant method (Barnes, 1965)
	– Not severely affected by deviation of certain points	– Accuracy may depends on the type of fitting algorithm, the cost function and the initial values of the parameters to be extracted	– the Newton–Raphson (Malaoui and Elmansouri, 2010)
	– More accurate (Ishaque et al., 2012)		– the quasi-Newton – method (Dennis and Moré, 1977) – Levenberg–Marquardt (LM) (Marquardt, 1963) – genetic algorithm (Ga) (Zagrouba et al., 2010) – simulated – annealing (SA) (Karamirad et al., May 2013; Almonacid et al., 2011) – the differential evolution (Siddiqui and Abido, 2013; Ishaque and Salam, 2011)

($n_1 = 1$) and 2 ($n_2 = 2$) depending of the model (one- or two-model) that is used. Furthermore, these values can be accepted only for an ideal cell; they become unsuitable for a real diode (Wolf and Benda, 2013). As reported by Wolf and Benda (2013) and Ishaque et al. (2011a) and adopted in this study, real solar cells present high values of ideality factor ($1 \leq n_1 \leq 2$ and $n_2 \geq 2$). Consequently we have fixed the initial values n_{10}, n_{20} of ideality factors to 1 and 2 respectively.

$$n_{10} = 1; n_{20} = 2 \qquad (2)$$

2.3.3. The diode saturation current

It is well accepted that the saturation current depends on the cell temperature and it can be expressed as function of temperature, short circuit current, and open circuit voltage (Ghani et al., 2013; Ishaque et al., 2011a).

$$I_{o0} = \frac{Isc_{ref}}{e^{\left(\frac{Voc_{ref}}{aVth_{ref}}\right)} - 1} \qquad (3)$$

where

$$Vth_{ref} = \frac{N_s k T_{ref}}{q} \qquad (4)$$

and

$$a = \begin{cases} n_{10} & \text{for one-diode models} \\ \frac{n_{10}+n_{20}}{p} & \text{for two-diode models} \end{cases} \qquad (5)$$

N_s is the number of cells connected in series in the module, k is the Boltzmann constant (1.38×10^{-23} J K^{-1}), q is the electron charge (1.6×10^{-19} C), T_{ref} the reference cell temperature, p is a coefficient which value is greater than 2.2 (Ishaque et al., 2011b).

According to Attivissimo et al. (2013), the initial value of the saturation current for each diode can be obtained by the following equation:

$$I_{o0i} = \frac{1}{2} \frac{Isc_{ref}}{e^{\left(\frac{Voc_{ref}}{n_{i0} \times Vth_{ref}}\right)} - 1}; i = 1, 2 \qquad (6)$$

2.3.4. The series and shunt resistances

In order to ensure good results the iteration process should be started with typically low initial low value for the two resistances (Attivissimo et al., 2013; Gow and Manning, 1999).

From the expression used in Wolf and Benda (2013) to compute R_s, one can deduce the initial value for this parameter according to the following equation:

$$R_s = n_0 \times \frac{Vth_{ref}}{I_2 - I_1} \times \log\left(\frac{Iph_0 - I_2}{Iph_0 - I_1}\right) - \frac{V_2 - V_1}{I_2 - I_1} \qquad (7)$$

where (V_2, I_2), (V_1, I_1) are two points on experimental I–V curve very close to the open circuit voltage point.

As the value of R_s is generally very low this parameter sometimes is neglected (Attivissimo et al., 2013). Hence, many authors assume that R_s can be initially fixed to zero.

Concerning the shunt resistance, Ishaque et al. (2011a) have proposed the following formula to calculate its initial:

$$R_{sh0} = \frac{Vmp_{ref}}{Isc_{ref} - Imp_{ref}} - \frac{Voc_{ref} - Vmp_{ref}}{Imp_{ref}} \quad (8)$$

3. Overview of the methodology

3.1. Description

The methodology developed in this paper enables to extract thanks to LM algorithm, the electrical parameters from the five selected models. First, an I–V curve is measured in fixed reference irradiation and temperature conditions (G_{ref}, T_{ref}) and then is used to determine the electrical parameters for the selected models. If the datasheet of the manufacturer is available, the I–V curve given under STC conditions can be considered. Otherwise, the outdoor current–voltage measurement of at least ten points can be performed. In that case, data should be measured quickly in such a way that the irradiation and the temperature can be considered constant. Then, a set of m points (V_i, I_i); $i = 1$: m (from the I–V curve) are derived and setup for the module.

To explain clearly the purpose of the calculation process, let us consider an electrical model characterized by n parameters p_i. We consider that the model is described by a function $L_P(V)$ where $p = (p_1, p_2, \ldots p_n)$ is a vector of the n parameters and V the voltage. For each voltage V_i, (given by the reference I–V curve in previous paragraph) the current calculated with the model is named Ith_i (theoretical current). Then, the absolute error vector which is the difference between the estimated and the measured currents can be written as follows:

$$r(p) = \begin{pmatrix} Ith_1(p) - I_1 \\ Ith_2(p) - I_2 \\ \\ \\ Ith_m(p) - I_m \end{pmatrix} \quad (9)$$

The objective here is to find the optimal vector p that minimizes the modulus $f(p)$ of the vector $r(p)$.

$$f(p) = \frac{1}{2} \sum_{j=1}^{m} [r_j(p)]^2 \quad (10)$$

The function $f(p)$ becomes the objective function to be minimized by the least squares and thanks to Levenberg Marquardt's algorithm.

Several statistical errors are used as indicators for the choice of the best model; they are calculated for all parameters of each model. Then, the electrical model which is considered to be the more effective, can be used in any simulation environment such as Simulink to estimate the electrical performance under real operating conditions of a PV module or generator. The calculations are done by considering the electrical parameters, the meteorological data of the site, the orientation and the tilt angle of the modules.

3.2. Statistical errors

The final theoretical current values obtained with the parameters calculated for each electrical model, are compared to experimental measurements by the mean of the following statistical errors: the standard deviation (SD), the root mean square error (NRMSE) and the normalized mean bias *error* (NMBE) (Malaoui and Elmansouri, 2010; Bouthevillain and Mathis, 1995). For each model, we also calculate the relative error (*ErPmax*) on the maximum power of the module in the reference conditions.

3.2.1. The standard deviation (SD) and the root mean square error (NRMSE)

The standard deviation (SD) and the root mean square error (NRMSE) given by Eqs. (11) and (12) respectively, provide information on the overall performance of the model. These two statistical errors, are used to compare term by term, the real difference between estimated and measured electric current. Generally, the more these two parameters are low, the more the model is efficient.

$$SD = \sqrt{\left(\frac{1}{m-1}\right) \times \sum_{i=1}^{m} (Ith_i - I_i)^2} \quad (11)$$

$$NRMSE = \frac{\sqrt{\left(\frac{1}{m}\right) \times \sum_{i=1}^{m} (Ith_i - I_i)^2}}{\left(\frac{1}{m}\right) \times \sum_{i=1}^{m} I_i} \quad (12)$$

3.2.2. The mean bias error (NMBE)

The NMBE indicator is given by the Eq. (13); it provides information on the overestimation or underestimation of the module performance. A positive value of NMBE implies an overestimation of values while negative values indicate an underestimation.

$$NMBE = \frac{\frac{1}{m}\sum_{i=1}^{m}(Ith_i - I_i)}{\frac{1}{m}\sum_{i=1}^{m} I_i} \quad (13)$$

3.2.3. The relative error (ErPmax) on the maximum power of the module

This error, expressed by the Eq. (14), gives the accuracy of the model. The maximum power is calculated from the optimal output parameters of the model. Then, this theoretical value is compared to the experimental power peak measured under the reference weather conditions.

$$ErPmax = \left| \frac{Pmax_{th} - Pmax_{measure}}{Pmax_{measure}} \right| \quad (14)$$

3.3. Updating of electrical parameters

Most of the electrical model parameters depend on the temperature and the solar irradiation. Once all these parameters are determined within reference conditions, their new values can be determined in any real operating

conditions (Siddiqui and Abido, 2013; Ma et al., 2014; Bai et al., 2014; Attivissimo et al., 2013; Ishaque et al., 2011a, 2011b), by using the following expressions (15)–(20).

3.3.1. The photocurrent I_{ph}

$$I_{ph}(G,T) = I_{ph_{ref}}\left[1 + \alpha_{I_{SC}}\left(T - T_{ref}\right)\right]\frac{G}{G_{ref}} \quad (15)$$

where T_{ref} and G_{ref} represent the solar cells temperature and solar irradiation respectively in reference condition. G and T are the same parameters in real operating conditions whereas $\alpha_{I_{SC}}$ is the temperature coefficient of the short-circuit current (available in the module data sheet). $I_{ph_{ref}}$ is the short-circuit current in the reference conditions.

3.3.2. The saturation current I_0

The values of the saturation current change with the cell temperature according to formula (16;17) and (18;19) for one-diode (Bai et al., 2014) and two-diode model (Attivissimo et al., 2013; Luque and Hegedus, 2003) respectively. Authors report that the formulas are suitable for all technology of silicon solar cells (Bai et al., 2014; Attivissimo et al., 2013; Luque and Hegedus, 2003).

$$I_0 = I_{0ref} \times \left(\frac{T}{T_{ref}}\right)^3 \times \exp\left(\frac{1}{k}\left(\frac{E_{g_{ref}}}{T_{ref}} - \frac{E_g(T)}{T}\right)\right) \quad (16)$$

$$\frac{E_g(T)}{E_{g_{ref}}} = 1 - 0.0002677\left(T - T_{ref}\right) \quad (17)$$

$$I_{0i} = I_{0ref} \times \left(\frac{T}{T_{ref}}\right)^{\frac{3}{n_i}} \times \exp\left(\frac{E_g(T)}{n_i.k}\left(\frac{1}{T_{ref}} - \frac{1}{T}\right)\right);$$
$$i = 1, 2 \quad (18)$$

$$E_g(T) = 1.17 - 0.000473\frac{T^2}{T + 636} \quad (19)$$

With I_{0ref}, I_0 the saturation current in reference and real conditions respectively; k is the Boltzmann constant in J K^{-1}. E_g [eV], the gap of the semi-conductor material in the real conditions is linked for one-diode model to the gap in reference conditions by expression (17) which has been widely used for silicon solar (Bai et al., 2014): The value of E_{gref} for the silicon solar cells at STC conditions is equal to 1.121 eV (Bai et al., 2014).

3.3.3. The series R_s and shunt R_{sh} resistance

Several formulas are reported in the literature (Bai et al., 2014; Gow and Manning, 1999) for calculation of R_s and R_{sh} values at non STC conditions from their reference values (data known at given conditions). In general, the formulas require material (semi-conductor) characteristic coefficients. These latters vary from one module to another and must be experimentally determined. To simplify the calculation, some authors assume that R_s is independent of incident irradiation and temperature for both one-diode models (Lun et al., 2013; Kulaksiz, 2013; Siddiqui and

Abido, 2013) and two-diode model (Attivissimo et al., 2013; Kaminski et al., 1999). Concerning the shunt resistance, it has been reported in the references (Siddiqui and Abido, 2013; Ma et al., 2014; De Soto et al., Jan. 2006) that it is inversely proportional to the solar irradiance. Later works (Attivissimo et al., 2013; Yordanov and Midtgard, 2011) have shown that this earlier assumption is true only at very low light intensities while R_{sh} is considered independent of temperature and can be set constant for $G > 100$ W/m^2. Unfortunately, these two assumptions lead to bad results with our modeling especially for two-diode models. It seems that the right way to determine R_s and R_{sh} should take into account the thermal parameters of the material. Nevertheless, the following formulas (Siddiqui and Abido, 2013; Ma et al., 2014; Bai et al., 2014) give good results for the two types of model:

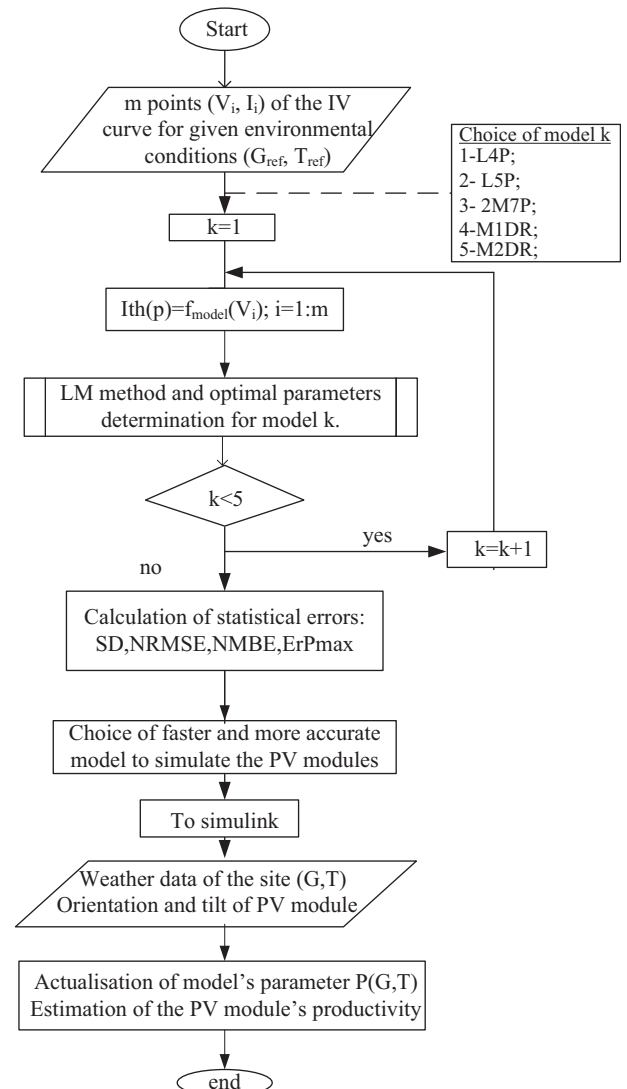$$\frac{R_s}{Rs_{ref}} = \frac{T}{T_{ref}}\left(1 - \beta \times ln\frac{G}{G_{ref}}\right) \quad (20)$$

Fig. 1. Synoptic view of the LM approach.

Table 3
Six different combinations of the methods used to estimate initial values of parameters.

	Case 0	Case 1	Case 2	Case 3	Case 4	Case 5	Case 6
I_{ph0}	2.8	Isc_{ref}	Isc_{ref}	Isc_{ref}	Isc_{ref}	Isc_{ref}	Isc_{ref}
R_{s0}	0.8	(Eq. (7))	(Eq. (7))	0	(Eq. (7))	(Eq. (7))	0
R_{sh0}	100	(Eq. (8))	(Eq. (8))	100	(Eq. (8))	(Eq. (8))	100
n_{10}	1	1	1	1	1	1	1
I_{10}	5.10^{-6}	(Eq. (3))	(Eq. (3))	(Eq. (3))	(Eq. (6))	(Eq. (6))	(Eq. (6))
n_{20}	2	2	2	2	2	2	2
I_{20}	5.10^{-6}	(Eq. (3))	(Eq. (3))	(Eq. (3))	(Eq. (6))	(Eq. (6))	(Eq. (6))

where β, is a coefficient which value is approximately 0.217 (Bai et al., 2014) and R_{Sref} the series resistance in the reference conditions.

$$R_{shref} = R_{sh} \cdot \frac{G}{G_{ref}} \qquad (21)$$

3.3.4. The cell temperature

The cell temperature is a function of the ambient temperature T_a and the solar irradiation G. It is generally approximated with the following expression (Bai et al., 2014; Alonso García and Balenzategui, 2004; Janna, 2000)

$$T = T_a + \frac{G}{800}(T_{NOCT} - 293.15) \qquad (22)$$

where T_{NOCT} is the nominal temperature of the PV cells at a solar irradiation of 800 W m^{-2}, an ambient temperature of 20 °C and a wind speed of 1 m s^{-1}. According to (Janna, 2000), using (22), the difference between the calculated and the measured temperature, is less than 3 °C.

Finally, by applying the previous formula, the most accurate model can be used in any simulation environment such as Simulink to predict the performance of PV modules from weather and solar data of a given site. The flowchart on Fig. 1 presents a synoptic view of the approach.

4. Results and discussions

4.1. Initial guesses

As mentioned above, the choice of initial guesses in iterative calculation methods is still a matter of debate. In this section, we analyze the sensitivity of different methods proposed in the literature to calculate the initial value of certain parameters. The authors of the methods and the corresponding formula are shown in Table 3. The calculation is performed for the five electrical models on three technologies of silicon modules (monocrystalline, multicrystalline and amorphous silicon); the same modules are studied in Section 4.3. The NRMSE is also determined for each electrical parameter and the number of iteration achieved for a given model is computed. The results depicted in Table 4 are derived from the combination of different proposals. The case 0 gives the best accuracy but the worst number of iteration; it is the contrary for the case 5 (the best number of iteration but worst accuracy). The best trade-off between the accuracy and rapidity is achieved for the case 1. Hence, all initial values of the parameters have been computed in the paper according to case 1.
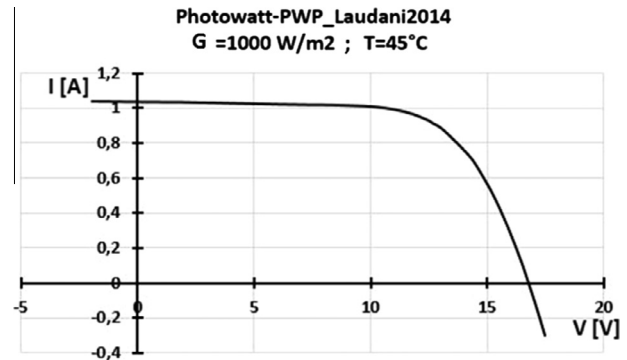

Fig. 2. Graph of experimental data (Laudani et al., 2014) plotted in Excel 2013.

Table 4
Sensitivity study of NRMSE and speed of calculation on the initial values of electrical models parameters.

	Case 0	CASE 1	Case 2	Case 3	Case 4	Case 5	Case 6
Sum of NRMSE							
sc-Si	7.66E−02	7.32E−02	1.03E−01	8.00E−02	1.02E−01	7.68E−02	7.68E−02
mc-Si	7.20E−02	7.24E−02	5.48E−02	8.64E−02	5.42E−02	5.45E−02	5.14E−02
a-Si	6.26E−02	1.16E−01	4.94E−01	1.04E−01	2.26E−01	3.47E−01	1.18E−01
Global	2.11E−01	2.62E−01	6.51E−01	2.71E−01	3.82E−01	4.78E−01	2.46E−01
Best to worst	1	3	7	4	5	6	2
Sum of the number of iterations							
sc-Si	4350	1807	4568	2489	788	2562	2562
mc-Si	4103	6077	2948	4072	2624	2784	4266
a-Si	3689	1494	2184	3846	5776	3592	4615
Global	12,142	9378	9700	10,407	9188	8938	11,443
Best to worst	7	3	4	5	2	1	6

4.2. Comparison with previous works

4.2.1. Determination of the initial set of points for an experimental I–V curve

As described above, an initial set of at least 10 points, must be provided at the beginning of the execution of the simulation. The best accuracy is obtained by using directly the experimental data. Nevertheless, if the measurements are not directly available, it is possible to use the data from the digitization of the I–V curves given in the manufacturers' datasheets. The curves can be digitized with Engauge software (a free software) or Un-Scan-It (not free but more accurate). We have performed a sensitivity study on the digitized curves. The results obtained with digitized curves are compared to those from experimental data. The study is based on experimental data reported in Laudani et al.

(2014). Our results are compared to those of Laudani et al. as their approach is also based on the LM algorithm. Data have been set as follow:

(1) Data 0: data (V_n, I_n) reported in Laudani et al. (2014).
(2) Data 1: data from the solution 1 developed by Laudani et al. (2014).
(3) Data 2: data obtained from our method with the experimental data (V_n, I_n) reported by Laudani et al. These data are then plotted with Excel and the graph is saved in JPEG format (see Fig. 2).
(4) Data 3: data obtained from our method by digitizing the I–V curve of Fig. 2 with Engauge software.
(5) Data 4: data obtained from our method by using the software Un Scan-It to digitize the I–V curve of Fig. 2.

Table 5
Comparison of different methods for obtaining the initial set of points.

L5P electrical model parameters	Solution 1 Laudani et al. (2014) (Data1)	Our study with Laudani direct measure (data2)	Our study after digitizing with Engauge	Our study after digitizing with Un-Scan-It
I_{ph} [A]	1.032173	1.031815	1.036851	1.035978
R_s [Ω]	1.218407	1.205414	1.111719	1.29706
R_{sh} [Ω]	783.516	845.998916	917.107338	731.218671
I_o [A]	3.0354E−06	3.30E−06	6.10E−06	2.01E−06
n	1.336752	1.345587	1.413751	1.295217
RMSE	2.12E−03	2.27E−03	3.84E−03	2.93E−03
Number of steps	12	164	237	190

Table 6
Manufacturers data of the five modules used in Siddiqui and Abido (2013) and Ma et al. (2014) at STC conditions ($G = 1000$ W m^{-2}, $T = 298$ K).

PV module	Previous work	Type	N_s	N_p	I_{sc} [A]	V_{oc} [V]	I_{mp} [A]	V_{mp} [V]
AP110	Siddiqui and Abido (2013)	mono-Si	36	1	7.50	20.7	6.60	16.7
SQ175	Ma et al. (2014)	mono-Si	72	1	5.43	44.6	4.95	35.4
S36	Siddiqui and Abido (2013)	mc-Si	36	1	2.30	21.4	2.18	16.5
KC-40T	Siddiqui and Abido (2013)	mc-Si	36	1	2.65	21.7	2.48	17.4
ST36	Siddiqui and Abido (2013)	CIS	42	1	2.68	22.9	2.28	15.8

Table 7
Parameters derived from L5P model by different methods for the five selected modules at STC.

Module	Study	I_{ph} [A]	R_s [Ω]	R_{sh} [Ω]	I_o [A]	n
AP110	Current study	7.5	0.152	66.831	1.65E−05	1.7
	Siddiqui and Abido (2013)	7.5118	0.0702	43.7946	1.64E−06	1.457
	Villalva et al. (2009)	7.516	0.0707	33.079	2.50E−07	1.3
SQ175	Current study	5.3463	0.6314	11691.82	1.30E−08	1.2125
	Ma et al. (2014)	5.449	0.7	196.2	1.20E−09	1.086
S36	Current study	2.2826	0.4574	7064.908	2.64E−07	1.4446
	Siddiqui and Abido (2013)	2.3113	1.0652	99999.99	2.067E−10	1.0006
	Villalva et al. (2009)	2.3015	0.5	769.4	4.29E−08	1.3
KC-40T	Current study	2.476	0.393	500.62	2.56E−08	1.271
	Siddiqui and Abido (2013)	2.6502	0.5239	7185.0838	5.568E−09	1.1748
	Villalva et al. (2009)	2.6511	0.3368	807.9666	3.850E−08	1.3
ST36	Current study	2.704	1.418	217.553	1.87E−05	1.807
	Siddiqui and Abido (2013)	2.7136	1.4725	117.6139	9.973E−7	1.4209
	Villalva et al. (2009)	2.711	0.5	43.1282	2.181E−07	1.3

(a)

AP110

(b)

AP110

Fig. 3. (a) I–V and (b) P–V curves for AP-110 monocrystalline silicon module.
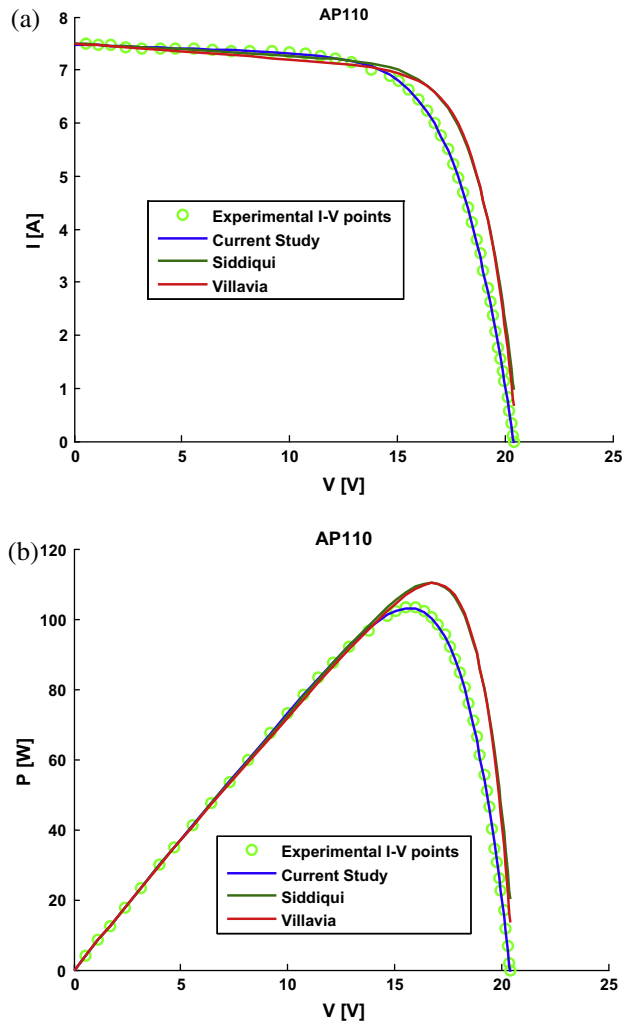
(a)

SQ175-PC

(b)

SQ175-PC

Fig. 4. (a) I–V and (b) P–V curves for SQ175-PC monocrystalline silicon module.

Then, the parameters obtained in each case are used in L5P model to recalculate the current intensity for the corresponding voltage of the experimental data (Laudani et al., 2014). In the three cases, the RMSE is computed with the formula 8 from Laudani et al. (2014). We also calculate the maximal relative error between the digitized data and the experimental data. The results are reported in Table 5.

The RMSE obtained with the direct use of the experimental data, is greater than that obtained by the approach of Laudani et al. but, it is lower than the previous works quoted in Laudani et al. (2014).

In general, based the values of RMSE and |ΔI|max, the results from the direct use of measurements are more accurate. Nevertheless, all of the data lead to an error less than 10 mA i.e. two significant decimal digits. Thus, we can conclude that, in the absence of data from direct measurements, the I–V curves in the datasheets of the manufacturers can be digitized in order to provide the initial points. However, more accurate is the digitizing tool, lower will be the error.
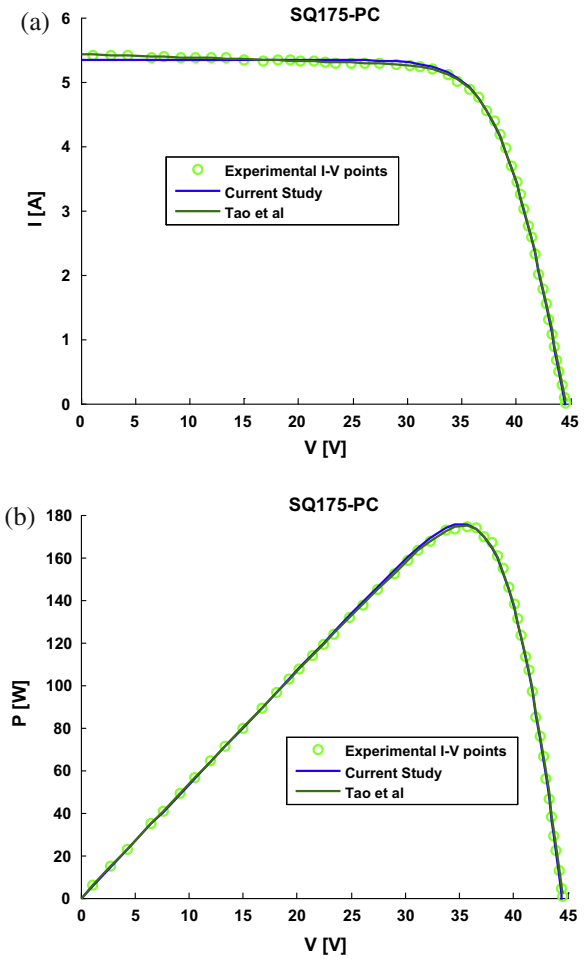
4.2.2. Comparison with other methods using the five parameters model (L5P)

In order to validate our approach, we have compare our results with those of three other methods reported in the literature. Modeling has been performed for five modules of different technologies that have been studied by Ma et al. (2014), Siddiqui and Abido (2013) or Villalva et al. (2009).

Below the three PV technologies concerned by the present study:

- two modules of monocrystalline silicon (mono-Si),
- two modules of multicrystalline silicon (mc-Si),
- one CIS (*Cooper Indium Selenium*) thin film module.

The details on the five modules characteristics at STC conditions are displayed in Table 6.

4.2.2.1. Method proposed by Siddiqui and Abido for the five parameters model. Siddiqui and Abido (2013) have developed a method for the five parameters L5P model. This method results from the combination of two evolutionary algorithms: the differential evolution (DE) and Tabu Search (TS) algorithms. The aim of their work was to
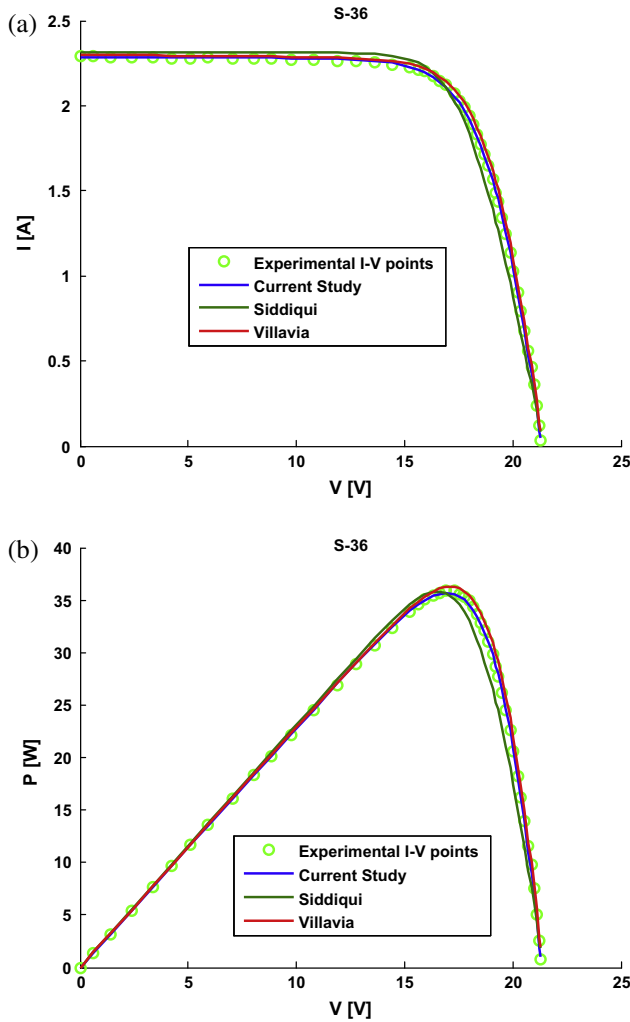
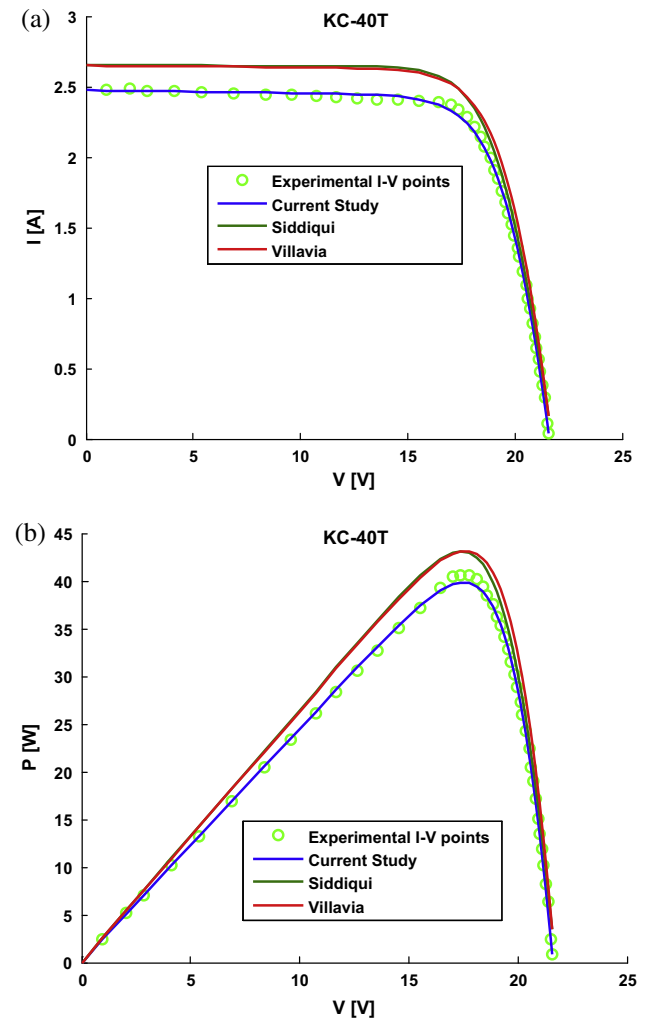Fig. 5. (a) I–V and (b) P–V curves for S-36 multi-crystalline silicon module.

Fig. 6. (a) I–V and (b) P–V curves for KC-40T multicrystalline silicon module.

determine the five parameters for a given PV module by considering its datasheet information obtained under STC conditions: the short-circuit current (I_{sc}), the open-circuit voltage (V_{oc}) and the maximal power point (V_{mp}, I_{mp}). For a given PV module, the hybrid algorithm (DE and TS) bring out the five parameters that minimize the following function called normalized error:

$$\text{Normalized error} = abs\left(\frac{I_{mp,mod} - I_{mp,exp}}{I_{mp,exp}}\right) + abs\left(\frac{V_{mp,mod} - V_{mp,exp}}{V_{mp,exp}}\right)$$

$$+ abs\left(\frac{I_{sc,mod} - I_{sc,exp}}{I_{sc,exp}}\right) + abs\left(\frac{V_{oc,mod} - V_{oc,exp}}{V_{oc,exp}}\right)$$

$$+ abs(I_{oc}) + abs\left(\frac{dP}{dV}\right)_{mp} \qquad (23)$$

4.2.2.2. Method proposed by Ma et al. for the five parameters model. To extract the five parameters, Ma et al. (2014) built six equations from datasheet specifications of the PV module. In addition to the five input parameters

used by Siddiqui and Abido, they use the temperature coefficient on the open circuit voltage β_{Voc}. Thus, they established a system of six equations that they solve with the non-linear equation solver, the fsolve function which set in Matlab by mean of the Levenberg–Marquardt method.

4.2.2.3. Parameter estimation for five parameters model by Villalva et al. (2009). In order to simplify the estimation methodology, Villalva et al. assume that the ideality factor is constant. Then, the other four parameters I_{ph}, R_s, R_{sh} and I_0, can be found out by minimizing the error on the maximum power.

4.2.3. Results of comparison and discussions
The three authors above-cited, have developed different methods of extraction of the L5P model. They are all based on the coordinates of three characteristic points of the PV modules under STC conditions available in the datasheets. The Table 7 shows under STC conditions, their results and those yielded by the LM approach.
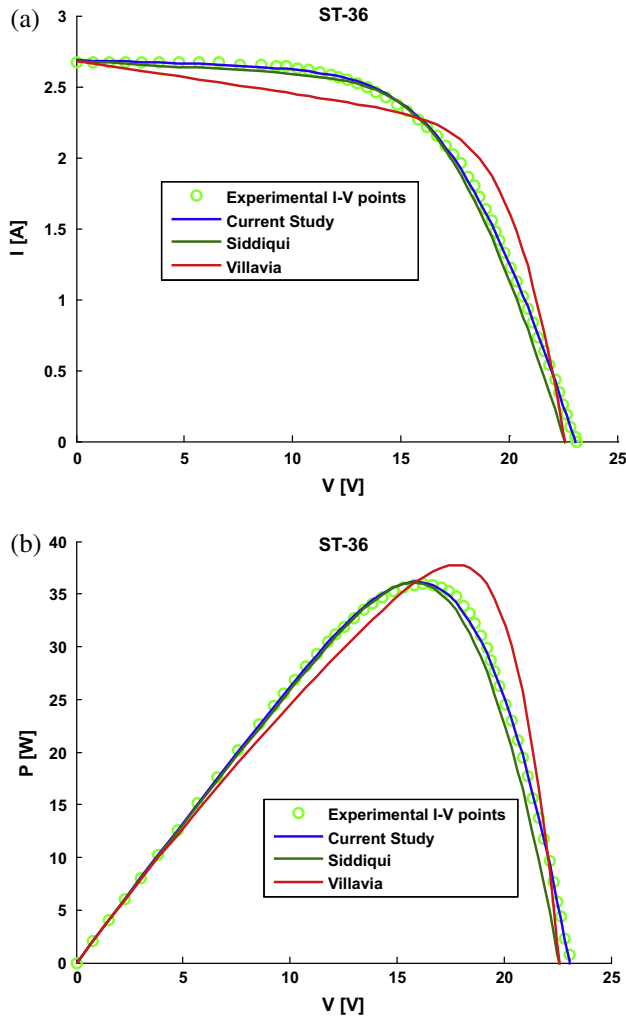
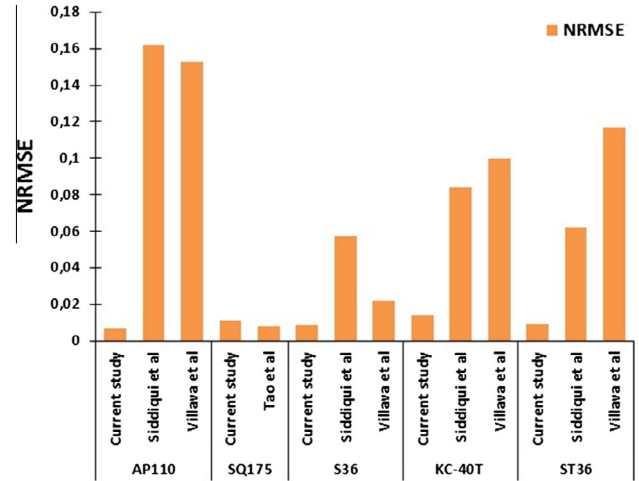Fig. 7. (a) *I–V* and (b) *P–V* curves for ST36 CIS module.

Fig. 8. Root-mean-square-error (NRMSE) on the *I–V* curve for different technologies of modules and estimation's method of L5P model parameters.
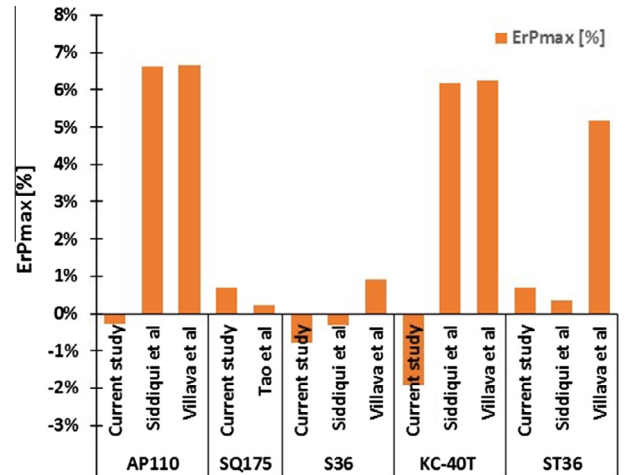

Fig. 9. Relative error in the estimation of the maximum power of the five modules by different methods of L5P parameters extraction.

Table 8
Template data of the four types of modules at STC.

Type of modules	N_s	P_{max} [Wp]	I_{sc} [A]	V_{oc} [A]
Monocrystalline (Bai et al., 2014) (mono-Si)	72	130	4.37	42.93
Multicrystalline REC230PEI (mc-Si)	60	230	8.3	37.1
Amorphous Bai et al., 2014 (a-Si)	36	103	5.11	29.61
HIT-N235SE10	72	235	5.84	51.8

To compare the methods, two steps were considered:

- for each PV module, the *I–V* curve under STC conditions (available on the datasheet) is used to determine the points (V_i, I_i) which are necessary for the modeling;
- then, the parameters obtained by each author (see Table 7) were used to estimate the values of intensity Ith_i, for a given voltage V_i. The couples (V_i, Ith_i) obtained with each extraction method, are compared to (V_i, I_i).

The implicit equation of L5P model was simply solved by the Matlab function fzero.

The Figs. 3–7 present the *I–V* and *P–V* curves generated by different methods for the L5P model. The experimental curves are represented by the circles and the modeling curves are plotted in full line. The root mean square error (NRMSE) and the relative error *ErPmax* are calculated once the parameters extraction is ended. NRMSE and *ErPmax* are shown on Figs. 8 and 9 respectively for all the methods.

An analysis of the experimental and the simulation graphs shows that the parameters obtained with the algorithm proposed here fit very well the *I–V* curves for all the modules (regardless of the technology) under STC. Furthermore, the results obtained with the methods of other authors generally deviate from the experimental data, some methods seem to be related to the module's technologies. In fact, over and beyond the electrical model, the characteristic parameters of the material can strongly
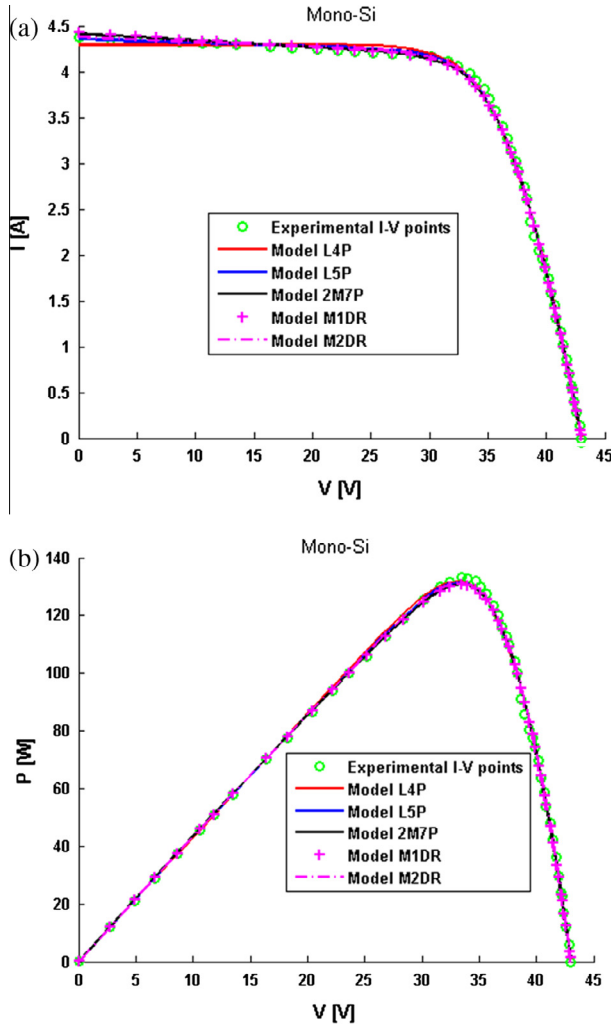
Fig. 10. (a) *I–V* and (b) *P–V* curves for mono-Si modules (Ghani et al., 2013) by five selected electrical models.

Fig. 11. (a) *I–V* and (b) *P–V* curves for REC230PEI module by five selected electrical models.

impact the curve so that an approximation set for a given technology could not be suitable to another one. For instance, the fixed value proposed by Villavia et al. for the ideality factor yields good results for monocrystalline and multicrystalline silicon module, while an unexpected *I–V* curve shape is obtained for thin film modules (CIS, Fig. 7). Such difference (between experimental and simulation results) can induce significant errors in the calculation of the PV module performance and consequently distort the output energy estimation.

Furthermore, according to the values of NRMSE (Fig. 8) and the relative error *ErPmax* (Fig. 9), for the monocrystalline module (SQ175-PC) our results are very similar to those obtained by Ma et al. (2014). On the other side, we have obtained better results compared to the curves given by Siddiqui and Abido (2013) and Villalva et al. (2009). In fact, the deviations observed with the methods of these two authors, especially for the modules AP110 and KC-40T (monocrystalline and multicrystalline silicon respectively) can be explained by the values of the performance parameters considered in their models. Indeed, for
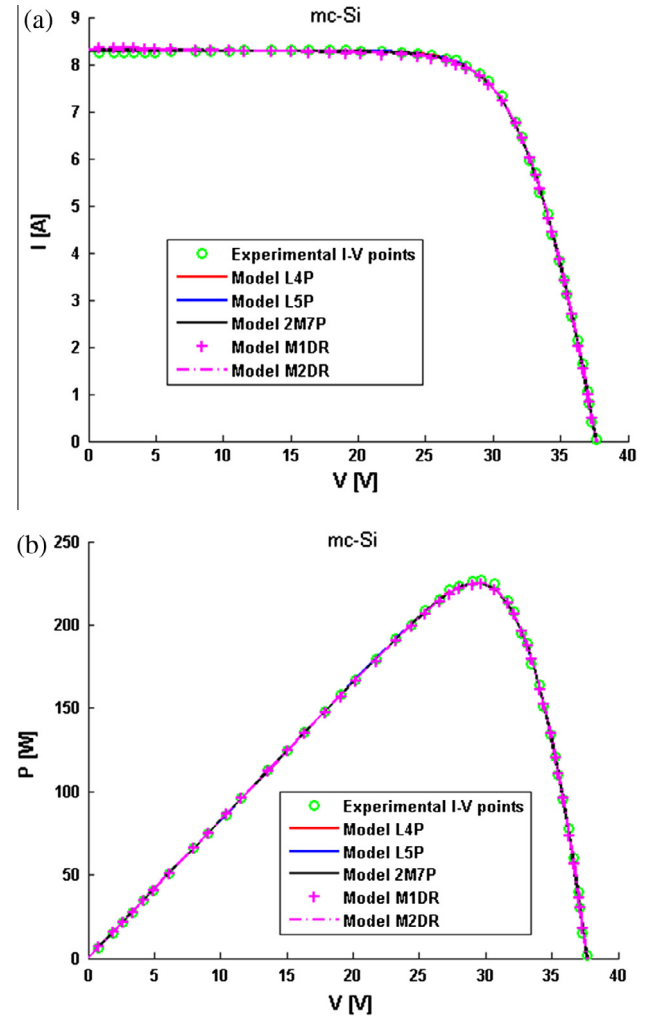
these two modules the values of the three parameters (short-circuit current, open circuit voltage and maximum power) given in the manufacturer datasheet table, are different from which can be read on the *I–V* curve available (in the same datasheet). They consider the table values whereas we use the whole *I–V* curve.

4.3. Results with five electrical models

In this part of the study, we compare the performance of five different electrical models listed in Table 1 for various technologies of silicon photovoltaic modules. The aim of this comparison is to find out an eventual classification of the models according to the PV technologies. Table 8 presents the characteristics of the modules selected.

The *I–V* curves of the modules given by the manufacturers under STC, were digitized to form the experimental measurement. Nevertheless, it is essential to take into account the three characteristic points of the *I–V* curve namely: $(0, I_{sc})$; $(V_{oc}, 0)$ and (V_{mp}, I_{mp}). Then, based on the experimental points we determined with the LM
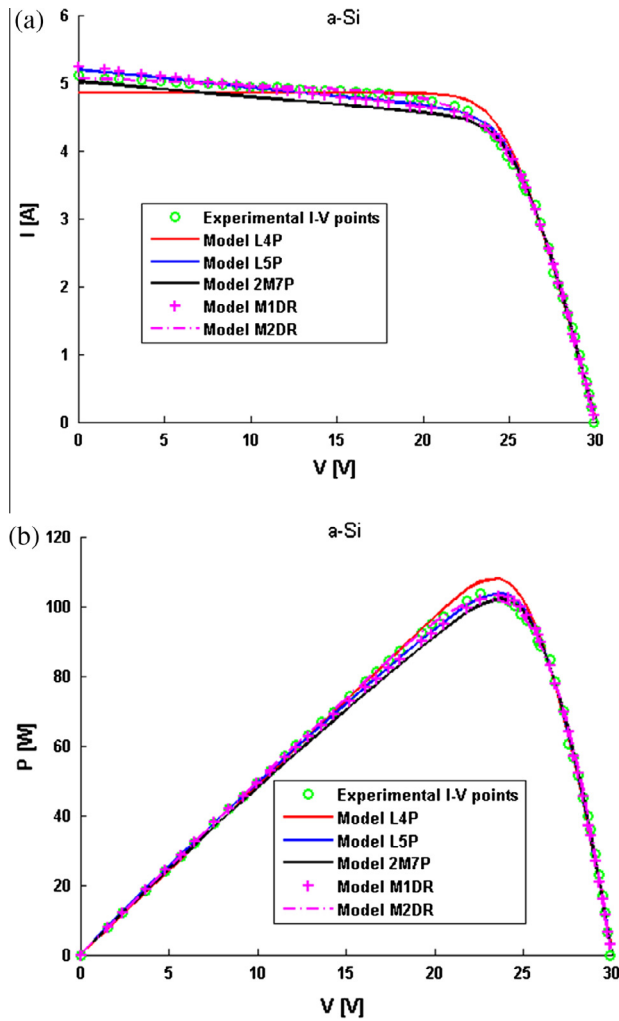
Fig. 12. (a) I–V and (b) P–V curves for (a-Si) module (Ghani et al., 2013) by five selected electrical models.
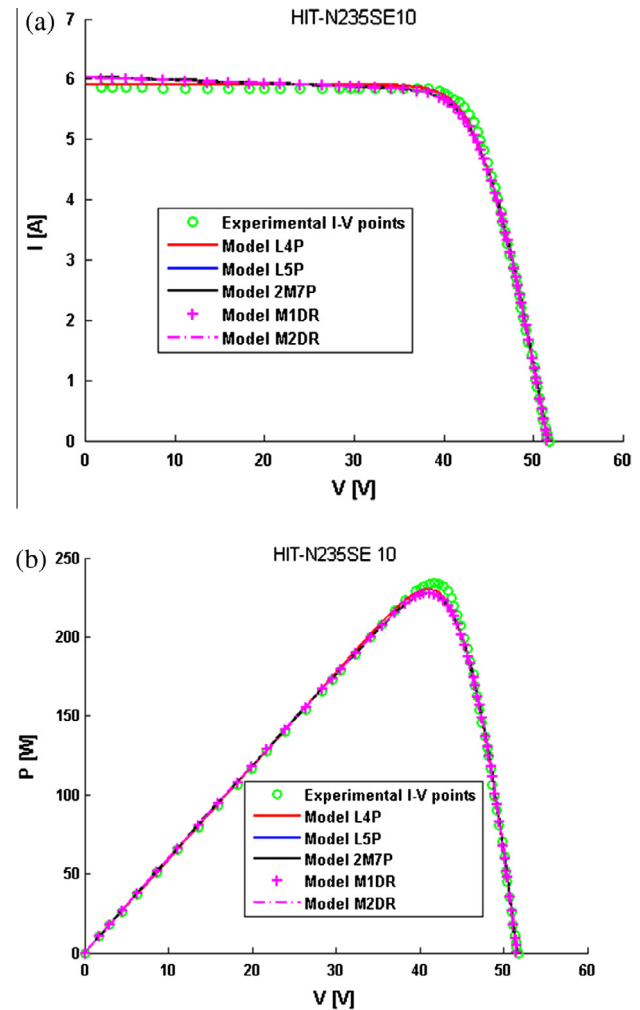

Fig. 13. (a) I–V and (b) P–V curves for HIT-N235SE10 module by five selected electrical models.

method, the parameters of the five different electrical models. The values of parameters found become the inputs of the corresponding model equations to plot the I–V and P–V curves of the module under STC (Figs. 10–13).

The performances of the different models are compared by considering three criteria:

- the ability to reproduce the I–V curve of the manufacturer under STC;
- the accuracy in the prediction of the maximum power point;
- the speed of calculation.

4.3.1. The ability to reproduce the I–V curve of the manufacturer under STC

This analysis is done thanks to the standard deviation (SD) and the root mean square error (NRMSE); the more both indicators are low, the more the model is efficient and accurate. Fig. 14 shows the histograms obtained for these two indicators.

When considering the five electrical models, it may be noted that the histograms show the same trend (Fig. 14). As SD and NRMSE seem to give the same information for a given module, only one of them should be sufficient to assess the effectiveness of the models. Furthermore, an overall view shows that the five models reproduce measurements (curves I–V under STC) with similar performance for the PV technology except a thin film model where a deviation is observed for L4P model. Indeed, the difference from one model to another for the same module is not significant. However, whatever the technology is, the L5P model gives the lower value. This justifies the use of the L5P model in most modeling works on photovoltaic cells and modules.

4.3.2. Estimation of the peak power of the module

This criterion may be proven as the backbone of several studies on photovoltaic systems including the prediction of module behavior and the implementation of maximum power point tracker (MPPT) device.
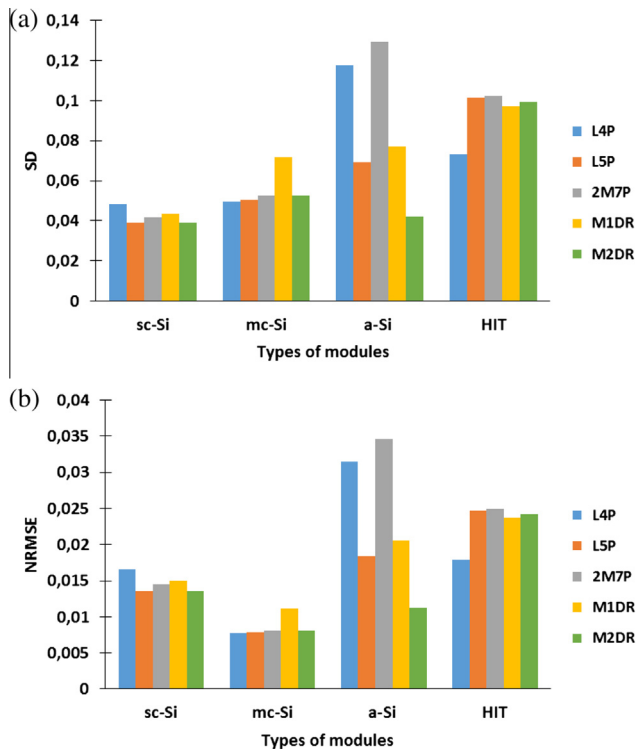
Fig. 14. SD (a) and NRMSE (b) for the four modules technologies and five electrical models.
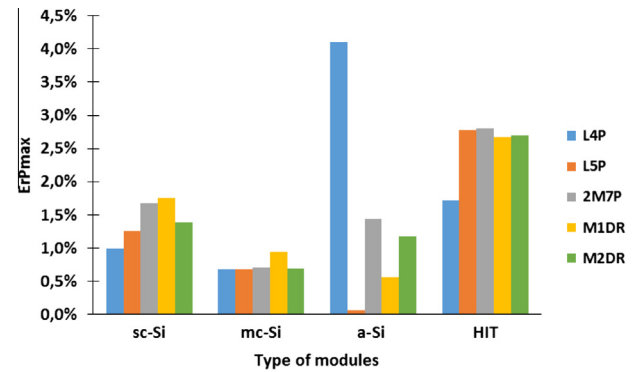

Fig. 15. Relative error from the models on the maximum power of the different technologies of PV modules.
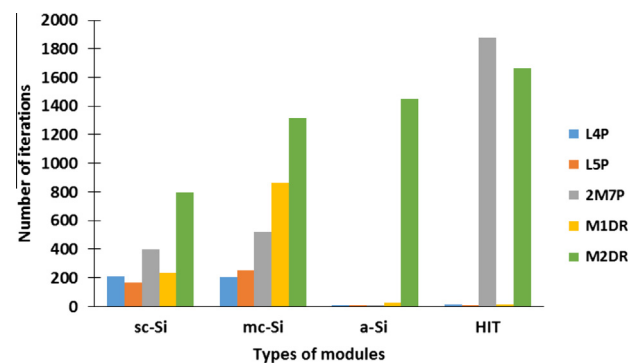

Fig. 16. Number of iterations performed by the LM algorithm to obtain the different model's parameters for four PV modules technologies.

Fig. 15 shows for each module, the relative error of the different models in estimating the peak power modules under STC. In summary, it appears that for all the technologies studied, models L4P and L5P better approximate the peak power of the modules except thin film technology for which the best fit is obtained with L5P model. However, as the difference with other models is low (around 4%), these two models can be used for tracking the optimum operating point of modules in the simulations.

4.3.3. Speed of calculation

As the accuracy does not present significant difference from one model to another, the speed of the modeling can be very critical for the choice of the best model. Here, the speed of the calculation is measured through the number of iterations. Fig. 16 shows the number of iterations required for convergence and thus the determination of the optimum parameters of each model. Due to its relatively low number of unknown parameters the model L4P is the fastest. And, as expected, it is closely followed by the model L5P. However, Fig. 16 shows another very important information: the link between the number of unknown parameters and the calculation speed is not always respected. L5P model (5 parameters) is faster than L4P (4 parameters) for sc-Si module and M2DR (8 parameters) is also faster than 2M7P (7 parameters) for HIT module.

If the choice only relies on model speed of calculation, we recommend the systematic use of electrical models L4P and L5P for all the PV module technologies.

4.4. Comparison of estimated and experimental energy production of a real PV plant

In order to verify the effectiveness of the LM method concerning the estimation of the energy production for a given PV plant, we used three photovoltaic fields installed on the experimental platform of our laboratory nearby Ouagadougou (capital of Burkina Faso). As shown on Fig. 17 the fields are connected to the electric grid via some SMA inverters. These inverters are equipped with a data logger for the collection of the energy production from the PV fields.

Each of the three fields consists of a single string of 24 PV modules. The installed modules, their cell technologies and the capacity of their field, are displayed in the Table 9.

As presented on Fig. 18, a model with Matlab/Simulink has been designed to simulate the behavior of a given PV module for temperature and solar irradiation in real conditions. A full equipped weather station (12°26′48″ North, 1°33′45″ West) nearby (around 500 m) the experimental platform measures several weather parameters such as the ambient temperature and the three components of solar irradiation namely: the Global Horizontal Irradiation (GHI), the Direct Normal Irradiation (DNI) and the Diffuse Horizontal Irradiation (DHI). The first unit of the Simulink model calculates the solar cells temperature and

(a)　　　　　　　　　　　　　　　　　　　　　(b)

Fig. 17. PV plant on the roof of our laboratory (LESEE, 2iE/Ouagadougou): (a) from right to left, monocrystalline, multicrystalline and HIT strings, (b): the corresponding network inverters.

Table 9
Characteristics of the three studied PV strings.

Reference of the modules	Cells' technologies	Power of PV field installed (kW p)
Sanyo HIT-N235SE10	HIT	5.64
REC230PEI	Multicrystalline	5.52
Sunmodule SW240 mono	Monocrystalline	5.76

the real incident radiation from the ambient temperature and the GHI. Then, the second unit estimates the I–V curve and the maximum power by using one of the five models described in Table 1 from the output results of the unit 1.

The simulation was performed with the site meteorological data of June 2012. The calculated maximum power can be used to evaluate, the monthly energy E_{th} in kW h:

$$E_{th} = N_{modules} \left(\frac{\sum P_{max} \times \Delta t}{1000} \right) \quad (24)$$

With $N_{modules}$, the number of identical modules of the PV field, P_{max} the instantaneous maximum power (in Wp) recorded during the simulation, and Δt the time step of the simulation which corresponds to the frequency of acquisition of weather data on the station.

The relative error $DeltaE$ regarding the energy measured is evaluated with the following expression:

$$DeltaE = \left(\frac{E_{meas} - E_{th}}{E_{meas}} \right) \times 100 \quad (25)$$

where E_{meas} is the value of energy measured by the inverters during the evaluation period.

The calculated results are compared to those measured and displayed in Table 10. These results confirm our view that, when the LM method is used, the modeling results are no longer dependent on the models. Thus, any of the five models can be used to predict the behavior of photovoltaic silicon modules in real environmental conditions. Indeed, by comparing the five models, it is observed that the maximum deviation of the relative errors is 1.79%, 3.42% and 3.27% for HIT, multicrystalline and monocrystalline technologies respectively. These differences are insignificant since the uncertainties of the maximum power measurement specified by the manufacturers are ranged from 5% to 10% of the peak power inscribed on the datasheets. Moreover, it should be noted that the maximum differences (relative error) between the measured and calculated values (14%, 12.05% and 7.26% respectively for monocrystalline, HIT and multicrystalline technologies) are achieved by M2DR models. The lowest relative errors (with measured data) are obtained by the L5P model for HIT (10.26%) and monocrystalline technologies (10.73%). The L4P model is slightly (0.08%) better than L5P model for multicrystalline technology. The discrepancies between the predicted and measured values correlate
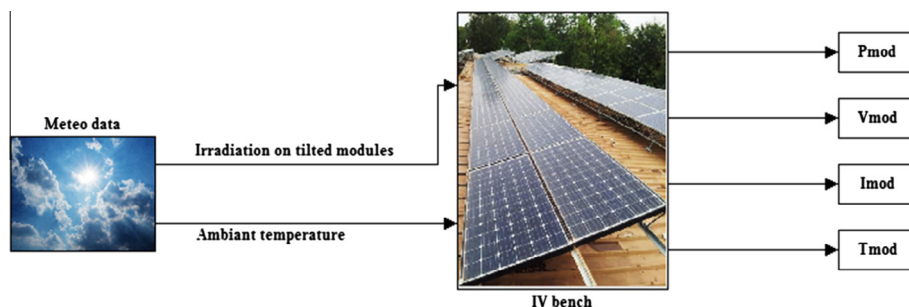

Fig. 18. Simulink model for simulation of PV module's behavior with different electrical models under real operating conditions.

Table 10
Comparison between the measured energy and calculated energy for two different technologies of PV field.

Electrical model	Field 1: 24 modules HIT of 235 Wp; P_{inst} = 5640 Wp			Field 2: 24 modules multicrystalline of 230 Wp; P_{inst} = 5520 Wp			Field 3: 24 modules monocrystalline of 240 Wp; P_{inst} = 5760 Wp		
	Energy [kW h]		Relative error (%)	Energy [kW h]		Relative error (%)	Energy [kW h]		Relative error (%)
	Measured	Calculated		Measured	Calculated		Measured	Calculated	
L4P	840.90	933.9215	11.06	802.96	833.7344	3.83	825.86	924,9492	12.00
L5P		927.1987	10.26		834.3523	3.91		914.4542	10.73
2M7P		941.2861	11.94		859.8918	7.09		937.0351	13.46
M1DR		927.8307	10.34		843.3945	5.03		920.6401	11.48
M2DR		942.2713	12.05		861.2334	7.26		941.4927	14.00

well with the orders of magnitude given by Rus-Casas et al. (2014). Indeed; theses discrepancies could be due to various power losses (Rus-Casas et al., 2014) (dirt and dust, shading, angular and spectral, ohmic, wiring system, junctions and mismatch between panels…), that are not taken into account in our calculations.

Nevertheless, it is now planned to take into account later on all these phenomena in order to improve the approach performed in this paper. To address this issue, a bench of outdoor characterization has been installed on the experimental platform of our laboratory and results from this platform will be exposed later in a coming paper.

5. Conclusion

In this paper, a new approach based on Levenberg Marquardt algorithm was developed. This method was used to extract the parameters of five different electrical models, selected among the most used in the literature. First, the problem of initial guess is considered. An analysis of several set of parameters lead to the choice of the group which offers the best trade-off between accuracy and speed of calculation. Then, the five parameters model (L5P) which is used by most authors has been considered to compare the LM approach to three other methods: a deterministic method and two heuristics methods. The results of this study show that, the precision achieved with LM method, is comparable to the deterministic method, but higher than that of the heuristics methods.

Furthermore, the method ability to replicate the performance of PV modules under STC has been analyzed for five electrical models implemented by the mean of LM algorithm. The study was performed on four modules of different technologies. It has been clearly noted that, when the LM method is used, the fives electrical models predict the behavior of the photovoltaic silicon modules with close accuracy in real environmental conditions. However, the best tradeoff between accuracy and calculation speed, is obtained with the five parameters model.

Finally, the theoretical estimation of solar energy production has been evaluated for three real power plants by using the five models considered in this paper. The maximum difference between calculated and measured energy is around 14%, 12.05% and 7.26% for the monocrystalline, HIT and multicrystalline technology plant respectively.

These differences could result from power losses due to multiple natural phenomena such as dirt and dust, shading, angular and spectral, ohmic, wiring system, junctions and mismatch between panels. An experimental study is ongoing in our laboratory to address the power losses on PV modules depending on the environmental realities of our climatic zones.

References

AIE. World Energy Outlook 2013. Paris: Organisation for Economic Co-operation and Development.

Almonacid, F., Rus, C., Pérez-Higueras, P., Hontoria, L., 2011. Calculation of the energy provided by a PV generator. Comparative study: conventional methods vs. artificial neural networks. Energy 36 (1), 375–384.

Alonso García, M.C., Balenzategui, J.L., 2004. Estimation of photovoltaic module yearly temperature and performance based on Nominal Operation Cell Temperature calculations. Renew. Energy 29 (12), 1997–2010.

Askarzadeh, A., Rezazadeh, A., 2012. Parameter identification for solar cell models using harmony search-based algorithms. Sol. Energy 86 (11), 3241–3249.

Attivissimo, F., Adamo, F., Carullo, A., Lanzolla, A.M.L., Spertino, F., Vallan, A., 2013. On the performance of the double-diode model in estimating the maximum power point for different photovoltaic technologies. Measurement 46 (9), 3549–3559.

Bai, J., Liu, S., Hao, Y., Zhang, Z., Jiang, M., Zhang, Y., 2014. Development of a new compound method to extract the five parameters of PV modules. Energy Convers. Manage. 79 (March), 294–303.

Barnes, J.G.P., 1965. An algorithm for solving non-linear equations based on the secant method. Comput. J. 8 (1), 66–72.

Bouthevillain, K., Mathis, A., 1995. Prévisions: mesures, erreurs et principaux résultats. Econ. Stat. 285 (1), 89–100.

Cañete, C., Carretero, J., Sidrach-de-Cardona, M., 2014. Energy performance of different photovoltaic module technologies under outdoor conditions. Energy 65 (February), 295–302.

De Soto, W., Klein, S.A., Beckman, W.A., Jan. 2006. Improvement and validation of a model for photovoltaic array performance. Sol. Energy 80 (1), 78–88.

Dennis, J., Moré, J., 1977. Quasi-newton methods, motivation and theory. SIAM Rev. 19 (1), 46–89.

Dongue, S.B., Njomo, D., Tamba, J.G., Ebengai, L., 2012. Modeling of electrical response of illuminated crystalline photovoltaic modules using four-and five-parameter models. Int. J. Emerg. Technol. Adv. Eng. 2 (11), 612–619.

Ghani, F., Duke, M., 2011. Numerical determination of parasitic resistances of a solar cell using the Lambert W-function. Sol. Energy 85 (9), 2386–2394.

Ghani, F., Duke, M., Carson, J., 2013. Numerical calculation of series and shunt resistance of a photovoltaic cell using the Lambert W-function: experimental evaluation. Sol. Energy 87 (January), 246–253.

Ghani, F., Duke, M., Carson, J., 2013. Numerical calculation of series and shunt resistances and diode quality factor of a photovoltaic cell using the Lambert W-function. Sol. Energy 91 (May), 422–431.

Gow, J.A., Manning, C.D., Development of a photovoltaic array model for use in power-electronics simulation studies. In: IEE Proceedings of Electric Power Applications, vol. 146, pp. 193–200.

Ishaque, K., Salam, Z., 2011. An improved modeling method to determine the model parameters of photovoltaic (PV) modules using differential evolution (DE). Sol. Energy 85 (9), 2349–2359.

Ishaque, K., Salam, Z., Syafaruddin, 2011a. A comprehensive MATLAB Simulink PV system simulator with partial shading capability based on two-diode model. Sol. Energy 85 (9), 2217–2227.

Ishaque, K., Salam, Z., Taheri, H., 2011b. Simple, fast and accurate two-diode model for photovoltaic modules. Sol. Energy Mater. Sol. Cells 95 (2), 586–594.

Ishaque, K., Salam, Z., Mekhilef, S., Shamsudin, A., 2012. Parameter extraction of solar photovoltaic modules using penalty-based differential evolution. Appl. Energy 99 (November), 297–308.

Janna, W.S., 2000. Engineering Heat Transfer. CRC Press, Boca Raton, Fla.

Kaminski, A., Marchand, J.J., Laugier, A., 1999. Methods to extract junction parameters with special emphasis on low series resistance. Solid-State Electron. 43 (4), 741–745.

Karamirad, M., Omid, M., Alimardani, R., Mousazadeh, H., Heidari, S.N., 2013. ANN based simulation and experimental verification of analytical four- and five-parameters models of PV modules. Simul. Model. Pract. Theory 34 (May), 86–98.

Kulaksiz, A.A., 2013. ANFIS-based estimation of PV module equivalent parameters: application to a stand-alone PV system with MPPT controller. Turk. J. Electr. Eng. Comput. Sci. 21, 2127–2140.

Laudani, A., Mancilla-David, F., Riganti-Fulginei, F., Salvini, A., 2013. Reduced-form of the photovoltaic five-parameter model for efficient computation of parameters. Sol. Energy 97 (November), 122–127.

Laudani, A., Riganti Fulginei, F., Salvini, A., 2014. High performing extraction procedure for the one-diode model of a photovoltaic panel from experimental *I–V* curves by using reduced forms. Sol. Energy 103 (May), 316–326.

Lun, S., Du, C., Guo, T., Wang, S., Sang, J., Li, J., 2013. A new explicit *I–V* model of a solar cell based on Taylor's series expansion. Sol. Energy 94 (August), 221–232.

Luque, A., Hegedus, S., 2003. Handbook of Photovoltaic Science and Engineering. Wiley, Hoboken, NJ.

Ma, T., Yang, H., Lu, L., 2014. Development of a model to simulate the performance characteristics of crystalline silicon photovoltaic modules/strings/arrays. Sol. Energy 100 (February), 31–41.

Malaoui, A., Elmansouri, A., 2010. Deux nouvelles méthodes complémentaires pour l'extraction optimale des paramètres électriques des jonctions. Rev. Energy Renouvelables 13 (2), 199–212.

Marquardt, D., 1963. An Algorithm for Least-Squares Estimation of Nonlinear Parameters. J. Soc. Ind. Appl. Math. 11 (2), 431–441.

Merten, J., Andreu, J., 1998. Clear separation of seasonal effects on the performance of amorphous silicon solar modules by outdoor measurements. Sol. Energy Mater. Sol. Cells 52 (1), 11–25.

Merten, J., Asensi, J.M., Voz, C., Shah, A.V., Platz, R., Andreu, J., 1998. Improved equivalent circuit and analytical model for amorphous silicon solar cells and modules. IEEE Trans. Electron. Dev. 45 (2), 423–429.

Merten, J., Sicot, L., Delesse, Y., de Montgareuil, A.G., 2008. Outdoor evaluation of the energy production of different module technologies. In Proceeding of the 23rd European Photovoltaic Solar Energy Conference Exhibition, pp. 2841–2845.

Muñoz, D., Razongles, G., Coignus, J., Merten, J., 2012. Novel equivalent circuit for heterojunction cells and diagnostic method based on variable illumination measurements (VIM). In: 27th Eur. Photovolt. Sol. Energy Conf. Exhib. October 2012, pp. 1268–1271.

Oueriagli, H.K.A., 1992. Analysis of dark current-voltage characteristics of Al/chlorophyll a/Ag sandwich cells. J. Appl. Phys. 11, 5523–5530.

Rus-Casas, C., Aguilar, J.D., Rodrigo, P., Almonacid, F., Pérez-Higueras, P.J., 2014. Classification of methods for annual energy harvesting calculations of photovoltaic generators. Energy Convers. Manage. 78 (February), 527–536.

Saloux, E., Teyssedou, A., Sorin, M., 2011. Explicit model of photovoltaic panels to determine voltages and currents at the maximum power point. Sol. Energy 85 (5), 713–722.

Sharafa, S.B., Akpootu, D.O., 2013. Extracting electrical parameters from semi-log plots of monocrystalline silicon PV module's normal operating IV data at a tropical station. Arch. Phys. Res. 4 (3), 23–30.

Siddiqui, M.U., Abido, M., 2013. Parameter estimation for five- and seven-parameter photovoltaic electrical models using evolutionary algorithms. Appl. Soft Comput. 13 (12), 4608–4621.

Townsend, T.U., 1989. A Method for Estimating the Long-term Performance of Direct-coupled Photovoltaic Systems. University of Wisconsin.

Villalva, M.G., Gazoli, J.R., Filho, E.R., 2009. Comprehensive approach to modeling and simulation of photovoltaic arrays. IEEE Trans. Power Electron. 24 (5), 1198–1208.

Wolf, P., Benda, V., 2013. Identification of PV solar cells and modules parameters by combining statistical and analytical methods. Sol. Energy 93 (July), 151–157.

Yordanov, G.H., Midtgard, O.-M., 2011. Physically-consistent parameterization in the modeling of solar photovoltaic devices. In: PowerTech, 2011 IEEE Trondheim, pp. 1–4.

Zagrouba, M., Sellami, A., Bouaïcha, M., Ksouri, M., 2010. Identification of PV solar cells and modules parameters using the genetic algorithms: application to maximum power extraction. Sol. Energy 84 (5), 860–866.